Pre-melting dynamics of DNA and its relation to specific functions

2009 J. Phys.: Condens. Matter 21 034107

(http://iopscience.iop.org/0953-8984/21/3/034107)

IOP PUBLISHING JOURNAL OF PHYSICS: CONDENSED MATTER

J. Phys.: Condens. Matter **21** (2009) 034107 (8pp) doi:10.1088/0953-8984/21/3/034107

REVIEW ARTICLE

Pre-melting dynamics of DNA and its relation to specific functions

Boian Alexandrov[1], **Nikolaos K Voulgarakis**[2], **Kim Ø Rasmussen**[1], **Anny Usheva**[3] **and Alan R Bishop**[1]

[1] Theoretical Division, Los Alamos National Laboratory, Los Alamos, NM 87545, USA
[2] Department of Chemical Engineering, University of California, Berkeley, CA 94720, USA
[3] Department of Medicine, Beth Israel Deaconess Medical Center and Harvard Medical School, Boston, MA 02215, USA

E-mail: arb@lanl.gov

Received 2 June 2008, in final form 3 September 2008
Published 17 December 2008
Online at stacks.iop.org/JPhysCM/21/034107

Abstract

We discuss connections between the nonlinear dynamics of double-stranded DNA, experimental findings, and specific DNA functions. We begin by discussing how thermally induced localized openings (bubbles) of the DNA double strand are important for interpreting dynamic force spectroscopy data. Then we demonstrate a correlation between a sequence-dependent propensity for pre-melting bubble formation and transcription initiation and other regulatory effects in viral DNA. Finally, we discuss the possibility of a connection between DNA dynamics and the ability of repair proteins to recognize ultraviolet (UV) radiation damage sites.

(Some figures in this article are in colour only in the electronic version)

1. Introduction

Understanding the function of DNA as a carrier of genetic information for life, health, and disease is one of the most important aspects of molecular biology. This understanding will not only provide answers to some of the mysteries of life, but will also help develop new therapeutic techniques for treating genetic diseases. Although, it has been known for decades that DNA is a highly dynamic system, it was commonly believed that the functional properties of DNA were determined primarily by the structure of the molecule. This is of course partially correct since the structure of DNA is designed to carry and protect the genetic code. However, it is now widely accepted that the dynamical conformational changes of DNA play a key role in some of its functions. For instance, in two of the most fundamental processes of life, transcription and replication, DNA has to locally open in order to allow the appropriate enzymes to engage and operate. In transcription the double strand is separated to allow the RNA polymerase to read the genetic code, while replication begins with a partial unzipping of the DNA end where DNA polymerase binds and starts assembling and reforming the molecule. Separation of the double strand of the DNA molecule is also important in biomedical techniques. In the polymerase chain reaction (PCR) for example, DNA double strands are routinely converted to separate single strands by melting at elevated temperature ($>80\,^{\circ}$C). This approach uses thermal energy to simply overwhelm the base pairing and base stacking interactions that stabilize the double helix at room temperature.

During these processes, DNA molecules undergo very large conformational changes and interact strongly with the environment (solution, proteins, drugs, etc). Nonlinearity cannot be ignored in a realistic representation of the dynamics of such complex processes. In addition, due to the large length and timescales at which the processes occur, the development of effective coarse-grained models are necessary. One of the most successful theoretical descriptions of DNA denaturation was proposed by Peyrard and Bishop [1] and Peyrard, Bishop, and Dauxois (PBD) [2]. The discrete and nonlinear nature of this model allows spontaneous formation of long lived localized openings (bubbles) over a substantial range of pre-melting temperatures. The extent and density of these openings increase with increasing temperature and finally results in a

complete dissociation of the molecule. Studies have shown that this simple model can quantitatively reproduce experimentally obtained melting curves of DNA. More recently studies have shown that the same model is capable of describing details (such as sequence and temperature dependence) of the bubble formation observed in experiments on relatively short (<100 base pairs) DNA fragments. This recent research has also provided strong indications that the DNA molecule is configured such that it favors formation of bubbles at the initiation sites for gene transcription, and thereby provides direction for its own transcription through bubble dynamics. Very recent studies have additionally demonstrated that the predictions of the PBD model are also in excellent agreement with experimental measurements of the mechanical unzipping of DNA.

Here we will review some of the statistical and dynamical properties of DNA within the PBD framework and discuss possible applications in molecular biology and biotechnology. Specifically, in section 2, we will briefly describe the PBD model. In sections 3 and 4 we will provide an overview of the theoretical prediction of bubble properties compared directly with the experiments on thermal and mechanical unzipping of DNA. In section 5 we discuss the reasons why the consideration of nonlinearity plays a central role in accurate descriptions of the denaturation of DNA. Having established that our modeling adequately describes bubble formation and dynamics, we devote the following sections 6 and 7 to discuss how the spontaneous occurrence of bubbles may relate to DNA functions such as transcription initiation and damage repair sites.

2. The Peyrard–Bishop–Dauxois model

The PBD model for double-stranded DNA was proposed, almost two decades ago [2], to describe the DNA denaturation transition. The model is highly nonlinear and simplified to only account for the two main effects dominating the physics underlying DNA denaturation. For each base pair, this model includes one degree of freedom y_n, the transverse stretching of the hydrogen bonds between complementary bases. In the PBD model, the potential energy, E, of a double strand of DNA of length N is

$$E = \sum_{n=1}^{N} [V(y_n) + W(y_n, y_{n-1})]. \tag{1}$$

Here $V(y_n) = D_n(1 - \exp[-\alpha y_n])^2$ represents the hydrogen bonds between complementary bases; $W(y_n, y_{n-1}) = \frac{k}{2}(1 + \rho \exp[-b(y_n + y_{n-1})])(y_n - y_{n-1})^2$ is the nearest-neighbor coupling that represents the (nonlinear) stacking interaction between adjacent base pairs: it is comprised of a harmonic coupling with a state-dependent coupling constant effectively modeling the change in stiffness as the double strand is opened (i.e. entropic effects). The heterogeneity of the sequence is incorporated by assigning different values to the parameters of the Morse potential, depending on the base pair type. For simplicity, however, we use the same value for the constants k, and ρ independently of the sequence. All parameters of this phenomenological model have been obtained from fitting experimental UV melting curves for a few short heterogeneous DNA sequences [3]. The specific parameter values obtained are $k = 0.025$ eV Å^{-2}, $\rho = 2$, $\beta = 0.35$ Å^{-1} for the inter-site couplings; for the Morse potential $D_{GC} = 0.075$ eV, $a_{GC} = 6.9$ Å^{-1} for GC base pairs, and $D_{AT} = 0.05$ eV, $a_{AT} = 4.2$ Å^{-1} for the AT base pairs.

3. Denaturation bubbles

It is known that sequence heterogeneity in DNA interplays with the entropy effects to create an extended pre-melting temperature window (including the biologically relevant regime), where large thermal bubbles are readily formed. The thermal effects driving the formation of denaturation bubbles, can be studied *in vitro* and provide important insight into biological processes. Recent experimental studies [4–6] have attempted to interrogate the nature and statistical significance of such bubble states. Innovatively, these experiments combine traditional UV absorption experiments with a bubble-quenching technique that traps ensembles of bubbles to capture statistical properties. In this section, we demonstrate how the PBD model successfully describes thermally generated bubbles by comparing our results with the recent experimental results reported in [5, 6].

Using standard Monte Carlo techniques, we have performed simulations of the PBD model applied to the specific sequences used in the above experiments. For each temperature, we performed a number of simulations. In each of these simulations, we compute the mean profile $\langle y_n \rangle$, from which we obtain the fraction of open base pairs. We consider the nth base pair to be open if $\langle y_n \rangle$ exceeds a certain threshold. Applying the same threshold, we record at the end of each simulation whether the entire molecule is open (denatured). Performing a large number of such simulations starting from different initial conditions, we obtain the average, fraction f of open base pairs and the average fraction of fully denatured molecules p at a given temperature. In this way, we directly simulate the experiments, where the measurements are made over a large ensemble of molecules.

In the same manner as [5], we obtain the averaged fractional length of the bubbles as $\langle l \rangle = (f - p)/(1 - p)$. In figure 1 we illustrate the performance of the model by showing our results for the sequence CCGCCAGCGGCGTTATTACATTTAATTCTTAAGTATTATAAGTAATATGGCCGCTGCGCC which is labeled (L60B36 in [5, 7]) in direct comparison with the experimental results on the same sequence. A very good agreement with the experimental results is observed. Specifically, we find as in the experimental results that $f \simeq l$ for 50 °C $< T <$ 65 °C, indicating the persistent existence of bubble openings in the equilibrium configurations of the molecule at these temperatures. At higher temperatures, l displays a plateau, resulting from the occurrence of completely denatured molecules at $T \simeq 75$ °C. As noted in the experimental work, the plateau occurs at $l \simeq 0.6$ because this is the ratio between the AT-rich central region, of 36 base pairs, and the molecule's total of 60 base pairs. Here we have, as an illustration, discussed

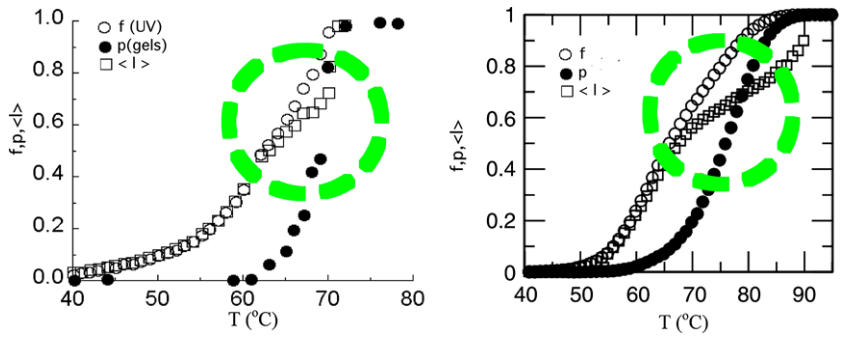

Figure 1. Experimental data (left) (reproduced from [5]) and results from simulations [7] (right) for the DNA sequence, CCGCCAGCGGCGTTATTACATTTAATTCTTAAGTATTATAAGTAATATGGCCGCTGCGCC. The circles indicate the temperature region of highest bubble activity.

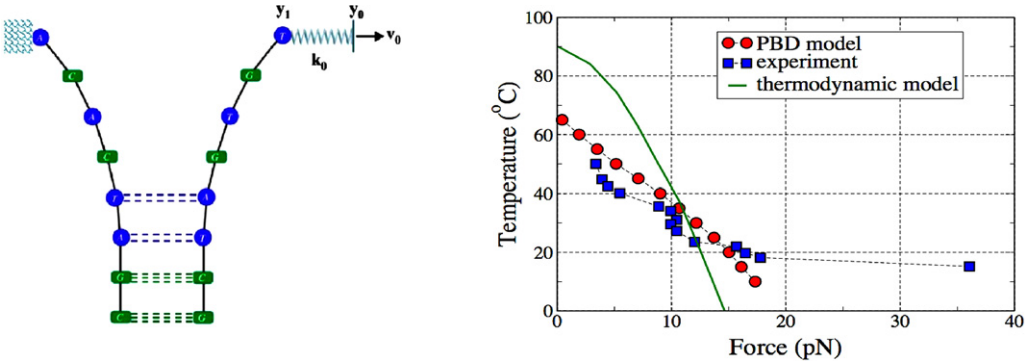

Figure 2. Schematic representation of the PBD model in a dynamic force spectroscopy experimental setting (left). Force–temperature phase diagram of λ-phage DNA. Squares correspond to the experimental results of [8]. Circles represent PBD-based simulations [9].

the comparison between the model and the experimental observations in the context of one specific sequence, however in the original work [7] the models have been compared to all the available experimental data which concerns several different sequences. The experimental observations regarding the nucleation size of the bubbles in the middle of a molecule and the possibility of a two-state transition are recovered by the model (see details in [7]). This demonstrates that the PBD model not only adequately describes the melting transition of very long DNA strands [2], but also provide a valuable description of the bubble formation in the pre-melting regime of shorter strands.

4. Forced unzipping of DNA

The development of single-molecule force spectroscopy and dynamical force spectroscopy has made possible the investigation of force-induced separation of double-stranded DNA at various temperatures [8]. Studying the force-induced separation of double-stranded DNA into single-stranded DNA is an important step towards understanding replication and transcription processes. It is also known that, in living organisms, the DNA separation is sometimes naturally driven by various enzymes and proteins, which can force apart the two strands of the double helix. In this sense the artificial force-induced separation of the double-stranded DNA is a tool to mimic and understand such processes.

For our purpose here the most essential aspect is the ability to understand the interplay between thermal bubble formation and applied unzipping forces. A first step towards understanding the relation between thermal denaturation and force-induced separation was taken by Danilowicz *et al* [8] who recently published the first experimentally determined phase diagram for DNA denaturation as a function of the applied force. The experimental data of this study showed, as expected, that the force required to unzip the DNA decreases with increasing temperature.

However, the detailed melting behavior, especially at higher temperatures where thermal denaturation bubbles play an increased role, is not immediately accessible from these experiments. Therefore, we applied the PBD model and a dynamical Monte Carlo technique to provide further insight into the mechanisms involved. In our simulations, as in the experiments, a force is applied by immobilizing one base and attaching a linear spring to the complementary base of the first base pair. The linear spring is assigned a stiffness k_0 such that the applied force is given by Hooke's law, $F_{\text{pull}} = k_0(y_0 - y_1)$, where y_1 and y_0 are the displacements (see figure 2 (left)) of the first base pair and the spring's opposite end point, respectively. The unzipping is then performed at a constant rate by moving the force probe by the distance Δ, $(y_0 \to y_0 + \Delta)$ after which N Monte Carlo steps are performed in order to compute the average displacement, $\langle y_1 \rangle$ of the first base pair. The force is subsequently calculated as $F_{\text{pull}} = k_0(y_0 - \langle y_1 \rangle)$. The

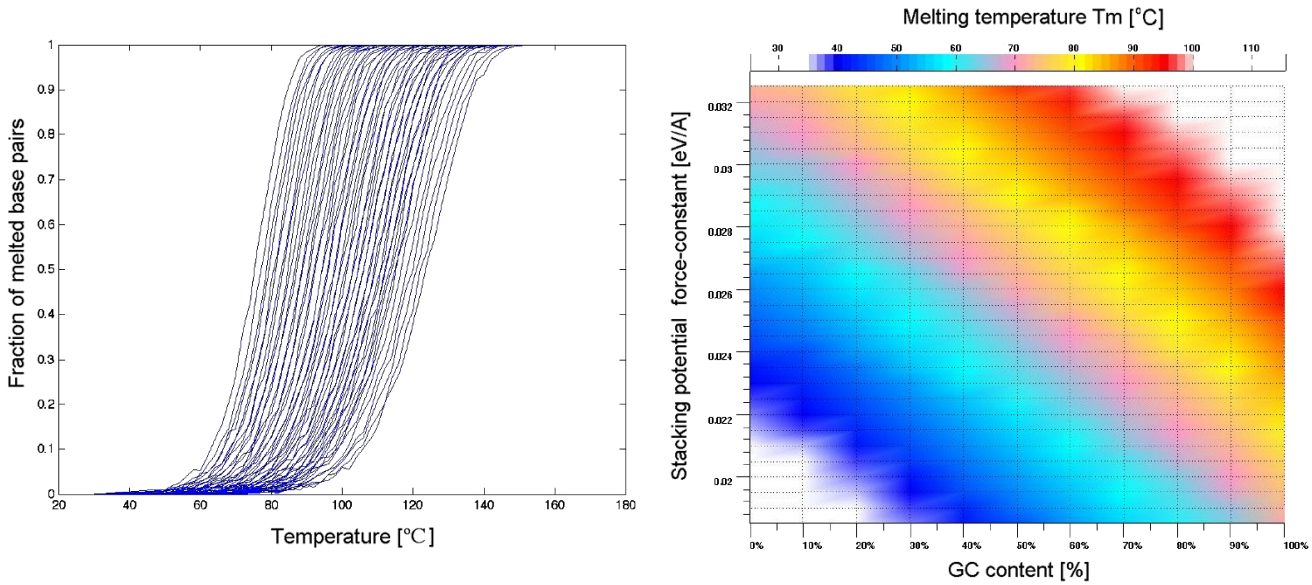

Figure 3. Left panel: simulated melting curves (fraction of the open base pairs) for a poly(GC) dsDNA sequence for several different values of the stacking-force constants. Right panel: dependence of the melting temperature (of a random sequence with controlled GC content) on both GC content and on the value of stacking constant [15].

more Monte Carlo steps used to determine $\langle y_1 \rangle$, the closer to equilibrium the system is before the next Δ move occurs such that the average pulling speed is $v_0 = \Delta/N$. Figure 2 (right) shows the experimental results (squares) [8], the theoretical result obtained with a popular thermodynamic model (green line) [8], together with our results (circles) from the described PBD simulations [9]. All results relate to the unzipping of λ-phage DNA (see [8, 9]) for sequence details). It can be seen that the data obtained with the PBD model are consistent with the experimental results in a far larger temperature range than the thermodynamic model. Particularly, at higher temperatures the thermodynamic model severely overestimates the required unzipping forces. This result can be attributed to the fact that the thermodynamic model neglects the spontaneous bubble formation [10]. The presence of thermal bubble formation leads to a considerable reduction of the measured force in the force-induced separation of the double-stranded DNA. This effect has also been observed in more sensitive measurements of DNA hairpin dynamics [11]. Again, the accuracy with which the PBD model reproduces the experimental result, throughout the temperature regime, strongly suggests that the bubble formation is accurately captured.

5. Stacking interactions

When the PBD model was first introduced [2], the calculations made with both molecular dynamic and transfer integral techniques clearly demonstrated the significant role that the stacking interactions have on the melting transition. Particularly, it was demonstrated that an effective nonlinear stacking interaction term is essential for adequately simulating the locally constrained nucleotide motion, resulting in long-range cooperative effects [12–14]. The role of this term in describing the melting transition has been noted early in the model development process [2], and the values of the relevant model parameters were chosen in order to reproduce a reasonable melting temperature for long homogeneous sequences [3]. In this sense the stacking constant k (see equation (1) and related discussion), represents an average value. Subsequently, the values of the remaining parameters β, D_{AT}, D_{GC}, a_{AT}, and a_{GC} have been obtained by fitting UV melting curves of a few short heterogeneous DNA sequences [3].

The stacking constant k has been left unchanged in the above process. It is, however, now well-established, experimentally and theoretically, that the stacking interaction plays an important role in DNA melting [16]. Similarly, studies [17] of *hyperthermophiles* (organisms that thrive in extremely hot (80–120 °C) environments), and *psychrophiles* (organisms capable of growing and reproducing in cold temperatures, below 15 °C), have made it clear that the existence of such organisms is possible only with the help of specific hot-active and cold-active enzymes, which are able to positively or negatively super-twist the DNA molecule. A DNA molecule that functions at normal physiological temperatures will begin to unfold and denature at temperatures well below 100 °C, and sustain no biological activity at temperatures below 15 °C. The existing hot-active and cold-active enzymes force the DNA to coil and twist, positively or negatively, making the molecule stable at high temperatures and flexible at low temperatures. It is clear that in such cases the hydrogen bonds are essentially unchanged, and therefore they do not play a role in changing the denaturation transition. The strength of the stacking potential in each of these cases is different, and again plays a role in defining the transition temperature.

Using a Monte Carlo technique and the protocol developed recently [7], we have investigated the dependence of the DNA melting on the value of the stacking constant k. We used

the PBD model to simulate dsDNA sequences with varying GC content. The results are presented in figure 3, where the left panel shows that the shape of the melting curves does not significantly depend on k, whereas it dramatically changes the melting temperatures. The right panel of figure 3 shows the calculated melting temperature of a random sequence with controlled GC content, versus k and it is clear that the melting temperature is quite sensitive to the value of k. The introduction of a neighbor-specific stacking constant, k_n, will therefore enable the sequence to sensitively control the local melting behavior. Based on such calculations, we used the data illustrated in figure 3 to determine values of the stacking constants for all possible combinations of neighboring base pairs. Our results will be published elsewhere [15].

6. Transcription and bubble formation

From the previous sections we conclude that double-stranded DNA is subject to temporary, localized openings of its two strands. At physiological temperatures, such thermally induced localized 'breathing' of the double-strand DNA, gives rise to localized DNA melting of ten base pairs or more, similar in size to some transcriptional bubbles [18]. The fact that the exact location and the evolution of these collective openings of consecutive base pairs are determined by the specific sequence then provides motivation to investigate whether transcription initiation and other regulatory sites possess an enhanced propensity for bubble formation. By comparing experimental results for the adeno-associated viral P5 promoter and for a P5 mutant promoter, that is known to be transcriptionally inactive, to the predictions of the PBD model, it was for the first time shown in [19, 20] that the most active regions strongly correlate with the transcriptional start site and other major regulatory sites.

To illustrate this, we reproduce the detailed results for the P5 promoter in figure 4. Figure 4 shows that for the P5 (wild-type) promoter we find a strong correlation between the transcription (labeled $+1$) start site and the occurrence of large (>10 base pairs) bubble openings. This correlation is further corroborated by S1 nuclease cleavage assays experiments, which, albeit crudely, indicate the regions most active in terms of thermally driven strand separation. For the P5 mutant promoter, the S1 nuclease cleavage assay experiments similarly corroborate the simulation results by the lack of any significant openings around the $+1$ site. Similar results were obtained for a number of other viral promoters [21, 22]. In particular, it was shown that the large bubbles containing the $+1$ base pair are also the longest lived (on average) bubbles [23].

7. UV radiation damages and melting

Experiments [24] have shown that DNA sequence mutations can change melting temperature, and the PBD model represents a suitable framework for investigating the effects of the damage and mutations on the DNA nonlinear dynamics.

We have numerically simulated the changes in the DNA dynamics in the presence of specific UV radiation damage. Ultraviolet light with a wavelength of 250 nm, promotes the formation of DNA dimers, making a rather strong connection between adjacent thymine bases (see

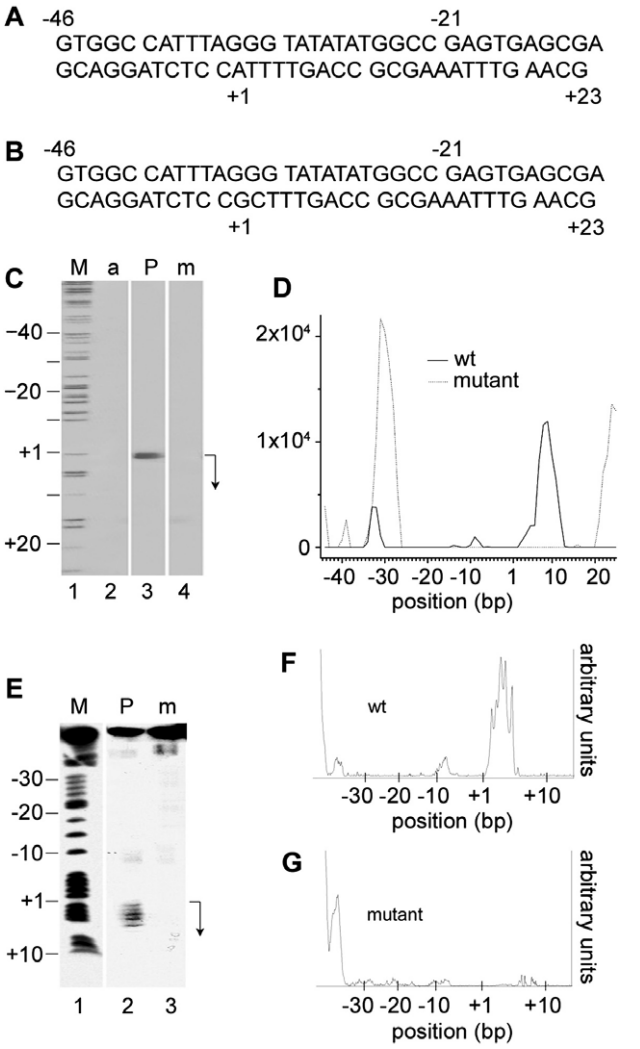

Figure 4. Analysis of P5 promoter and P5 mutant promoter. (A) Upper strand, sequence of the 69 base pair (bp) P5 core promoter. (B) Upper strand, sequence of the 69 bp mutant P5 promoter. (C) Transcription assay on a 120 bp fragment containing the P5 promoter and P5 mutant fragment in a nuclear extract. The arrow on the right indicates the transcription start site and the direction of transcription. The corresponding sequence position is indicated to the left of the marker. Lane 1, GA DNA sequencing reaction was used as a marker (M); lane 2, transcription from the P5 promoter with a-amanitin (a); lane 3, RNA transcription products with P5 promoter (P); lane 4, RNA transcription products from the P5 mutant template (m). (D) PBD simulation of the P5 sequence, plotting simulated instances of 2.1 Å-separated openings of 10 bp or more versus the base position in the sequence. The solid line represents the results of the wild-type P5 promoter, and the broken line represents results with the mutant P5 promoter sequence. (E) S1 nuclease cleavage of the P5 promoter and the P5 mutant promoter. The corresponding sequence position is indicated to the left of the panel. Lane 1, lower strand-labeled P5 promoter GA sequencing reaction (M); lane 2, P5 promoter S1 cleavage reaction (P); lane 3, P5 mutant promoter cleavage reaction (m). (F) Cleavage density profile of the wild-type (wt) P5 promoter DNA in the S1 nuclease experiment. (G) Cleavage density profile of the mutant P5 promoter DNA in the S1 nuclease experiments.

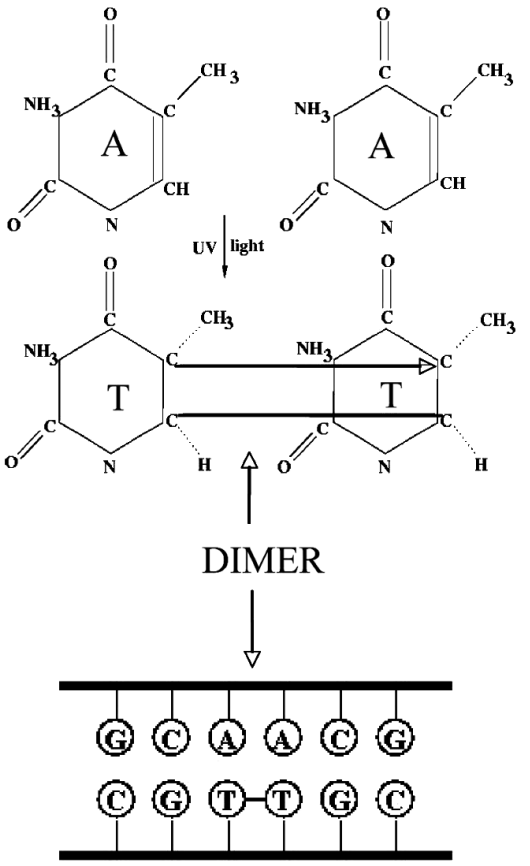

Figure 5. Schematic diagram of the quasi-stable dimer configuration created by 250 nm ultraviolet light.

figure 5). If left unrepaired, these dimers may induce skin cancer. This UV dimer formation (figure 5), causes adjacent thymine base pairs to form a strong covalent bond, while the pairing of the complementary adjacent adenines is weakened. This weakening in turn causes a 13 K decrease of the melting temperature of the double-stranded octamer d(GCGTTGCG)d(CGCAACGC) in the presence of a UV dimer [25]. Using the PBD model and a constrained Monte Carlo algorithm [26], the parameters of the PBD model were adjusted so as to reproduce this change in melting temperature for the octamer d(GCGTTGCG)d(CGCAACG) [27]. An 11% reduction in the dissociation energy, D_n, of the relevant Morse potential was observed to be necessary to obtain the 13 K reduction in the melting temperature (see melting curves in figure 6). Besides weakening of the interaction between the adjacent adenines, the UV dimer plays the role of a structural 'impurity' in the DNA sequence, and therefore effectively changes the stacking interaction between the adjacent thymine base pairs. This impurity's role, also decreases the spatial and temporal coherence length of the fluctuations, and enhances the decrease of the melting temperature.

A random sequence of 64 base pairs was generated and the same octamer, with and without the presence of a UV dimer, was inserted in the middle of this sequence. The same Monte Carlo technique was applied to this new sequence, and the average displacements from the equilibrium positions

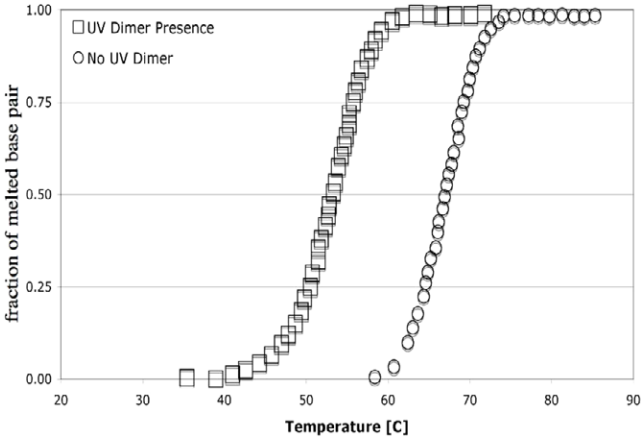

Figure 6. Simulated melting curves of the octamer d(GCGTTGCG)d(CGCAACG). The circles show the melting behavior for the unaltered sequence, while squares indicate the behavior when the UV-dimerization has occurred.

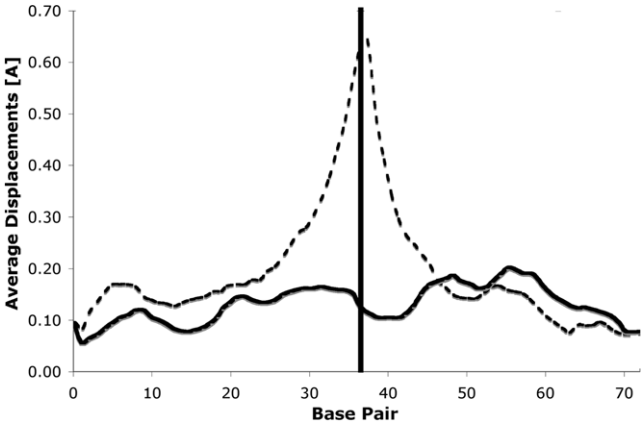

Figure 7. Average strand displacement of DNA with a dimer (dashed line) and without a dimer (solid line) showing the enhanced opening in the dimer neighborhood at 37 °C. The solid vertical line indicates the position of the UV dimer.

were obtained (see figure 7). In figure 7, a three- to four-fold increase is evident in the relative displacements between the base pairs belonging to the two opposite strands at the dimer position, in comparison with the case where there is no UV dimer in the sequence. The DNA sequence was also investigated with Langevin molecular dynamics. In this case the dimer presence was taken into account using a Lagrange multiplier. In figure 8, the probability for an opening larger than a given threshold is shown. It can be seen that the probability for the occurrence of large bubbles at the dimer position is approximately 25 times larger than the probability in the absence of a dimer. Finally, the data presented in [27] indicate that there are significant changes in the spatio-temporal characteristics of double-stranded DNA upon UV dimer formation between adjacent thymine base pairs. We suggest that this changed dynamics may be part of enabling the repair proteins to rapidly detect the occurrence of radiation damage.

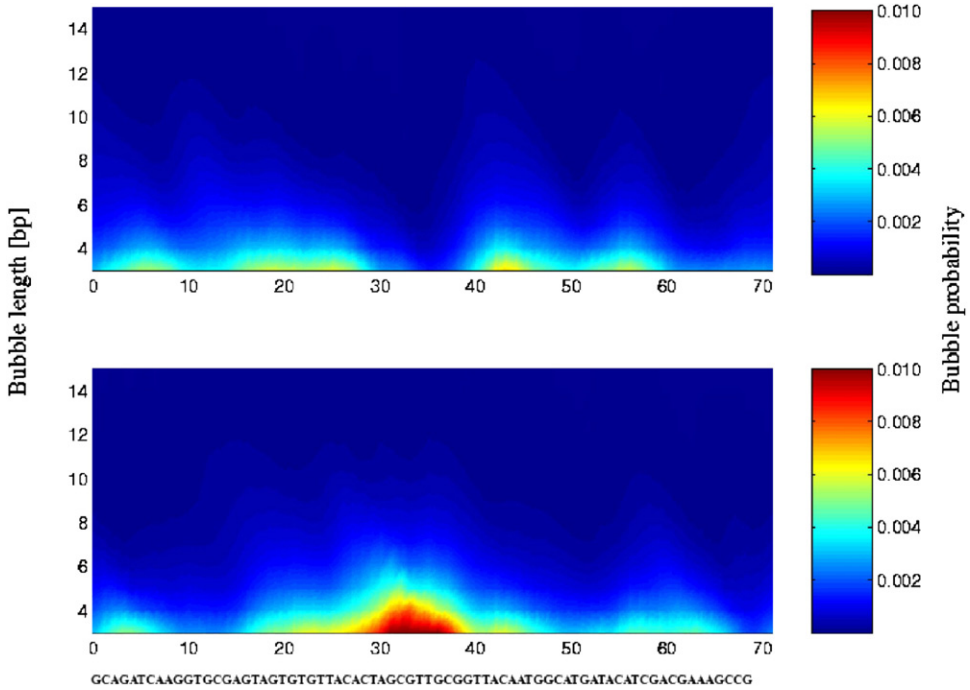

Figure 8. The probability for bubbles with amplitude above 1.5 Å as a function of bubble position and bubble length. The upper panel represents this probability without a UV dimer, and the lower panel represents the probability with a UV dimer present, both at 37 °C.

8. Conclusions

DNA is a remarkable vehicle for studies of nonlinear phenomena. Its structure and dynamics are rich yet remain simpler than those of proteins and other biological macromolecules. DNA embodies fundamental nonlinear science questions. Particularly, how do the sequence and nonlinearity interplay to determine the nature of the localized excitations (bubbles)? DNA exhibits very large amplitude fluctuations, which are essential for biological functions, and can be studied experimentally with many tools; DNA can be meaningfully described by simple models, which are amenable to studies applying nonlinear dynamical systems techniques. We have summarized here that modeling of DNA, with only a single degree of freedom per base pair gives valuable results capturing essential dynamical features of the molecule. Our studies strongly suggest that this level of modeling even has biological relevance, by providing a method for sequence screening that may be able to exhibit structures which are not detected by usual methods based on a bioinformatic analysis of the sequence. We believe that this kind of meso-scale modeling, with a strong coupling to experiments, has the potential to enable significant insight into several of DNA's biomolecular functionalities. Very interestingly, the notion that strong local dynamic deviations from 'average' or 'homogeneous' structures are essential for determining function is now a major topic of research in many hard and soft materials (organic [28] and inorganic [29, 30]), and increasingly in biological matter [31–33], with nonlinearity and bonding constraints the likely source [34, 35], and discrete breathers (as here) very natural realizations. Importantly, these functional heterogeneities are *equilibrium* properties, used for specific functions, very much in the spirit of the 'landscapes', introduced by Frauenfelder [36] and others for macromolecules such as myoglobin. Adapting the global structure of the same protein for distinct functions through specific local distortions is clearly appealingly efficient from a biological evolutionary perspective.

Acknowledgments

We gratefully acknowledge our collaborators who have co-authored the original work that we have summarized here. This work was carried out under the auspices of the National Nuclear Security Administration of the US Department of Energy at Los Alamos National Laboratory under contract No. DE-AC52-06NA25396.

References

[1] Peyrard M and Bishop A R 1989 *Phys. Rev. Lett.* **62** 2755
[2] Dauxois T, Peyrard M and Bishop A R 1993 *Phys. Rev.* E **47** R44
[3] Campa A and Giansanti A 1998 *Phys. Rev.* E **58** 3585
[4] Montrichok A, Gruner G and Zocchi G 2003 *Europhys. Lett.* **62** 452
[5] Zeng Y, Montrichok A and Zocchi G 2003 *Phys. Rev. Lett.* **91** 148101
[6] Zeng Y, Montrichok A and Zocchi G 2004 *J. Mol. Biol.* **339** 67
[7] Ares S, Voulgarakis N K, Rasmussen K Ø and Bishop A R 2005 *Phys. Rev. Lett.* **94** 035504
[8] Danilowicz C, Kafri Y, Conroy R S, Coljee V W, Weeks J and Prentiss M 2004 *Phys. Rev. Lett.* **93** 078101
[9] Voulgarakis N K, Redondo A, Bishop A R and Rasmussen K Ø 2006 *Phys. Rev. Lett.* **96** 248101

[10] Nelson D R 2006 *NATO Science Series II: Mathematics, Physics and Chemistry* vol 160 (New York: Springer-Verlag) p 65 and references therein
[11] Hanne J, Zocchi G, Voulgarakis N K, Bishop A R and Rasmussen K Ø 2007 *Phys. Rev.* E **76** 011909
[12] Voulgarakis N K, Kalosakas G, Rasmussen K Ø and Bishop A R 2004 *Nano Lett.* **4** 629
[13] Kalosakas G, Rasmussen K Ø and Bishop A R 2004 *Synth. Met.* **141** 93
[14] Kalosakas G, Rasmussen K Ø and Bishop A R 2006 *Chem. Phys. Lett.* **432** 291
[15] Alexandrov B S, Gelev V, Usheva A, Bishop A R and Rasmussen K Ø 2008 in preperation
[16] Allawi H T and SantaLucia J Jr 1997 *Biochemistry* **36** 10581
[17] Daphne G, Benjamin D, Vinciane B, Depiereux E, Uversky E V, Gerday C and Feller G 2003 *J. Biol. Chem.* **278** 37015
[18] Gueron M, Kochoyan M and Leroy J L 1987 *Nature* **328** 89
[19] Choi C H, Kalosakas G, Rasmussen K Ø, Hiromura M, Bishop A R and Usheva A 2004 *Nucl. Acids. Res.* **32** 1584
[20] Kalosakas G, Rasmussen K Ø, Bishop A R, Choi C H and Usheva A 2004 *Europhys. Lett.* **68** 127
[21] Rapti Z, Smerzi A, Rasmussen K Ø, Bishop A R, Choi C H and Usheva A 2006 *Europhys. Lett.* **74** 540
[22] Rapti Z, Smerzi A, Rasmussen K Ø, Bishop A R, Choi C H and Usheva A 2006 *Phys. Rev.* E **73** 51902
[23] Alexandrov B S, Wille L T, Rasmussen K Ø, Bishop A R and Blagoev K 2006 *Phys. Rev.* E **74** 50901
[24] Montgomery J, Wittwer C T, Palais R and Zhou L 2007 *Nat. Protoc.* **2** 59
[25] Kemmink J, Boelens R, Koning T, van der Marel G A, van Boom J H and Kaptein R 1987 *Nucl. Acids Res.* **15** 4645
[26] Fixman M 1974 *Proc. Natl. Acad. Sci. USA* **71** 3050
[27] Blagoev K B, Alexandrov B S, Goodwin E H and Bishop A R 2006 *DNA Repair* **7** 863
[28] Tretiak S, Saxena A, Martin R L and Bishop A R 2003 *Proc. Natl. Acad. Sci. USA* **100** 2185
[29] Bishop A R, Lookman T, Saxena A and Shenoy S R 2004 *Europhys. Lett.* **63** 289
[30] Ahn K, Lookman T and Bishop A R 2004 *Nature* **428** 401
[31] Volkman B F, Lipson D, Wemmer D E and Kern D 2001 *Science* **291** 2429
[32] Ming D and Wall M E 2005 *Phys. Rev. Lett.* **95** 198103
[33] Juanico B, Sanejouand Y-H, Piazza F and De Los Rios P 2007 *Phys. Rev. Lett.* **99** 238104
[34] Thorpe M F, Jacobs D J, Chubynsky M V and Phillips J C 2000 *J. Non-Cryst. Solids* **266** 859
[35] Barre J, Bishop A R, Lookman T and Saxena 2005 *Phys. Rev. Lett.* **94** 208701
[36] Frauenfelder H, Sligar S G and Wolynes P G 1991 *Science* **254** 1598